

# The global phase diagram of the one-dimensional SYK model at finite $N$

Xin Dai,<sup>1</sup> Shao-Kai Jian,<sup>1</sup> and Hong Yao<sup>1,2,\*</sup>

<sup>1</sup>*Institute for Advanced Study, Tsinghua University, Beijing 100084, China*

<sup>2</sup>*State Key Laboratory of Low Dimensional Quantum Physics, Tsinghua University, Beijing 100084, China*

(Dated: December 3, 2024)

We study the generalized Sachdev-Ye-Kitaev (SYK) chain consisting of  $N$  (complex or Majorana) fermions per site with random interactions and hoppings between neighboring sites. In the limit of vanishing SYK interactions, from both supersymmetric field theory analysis and numerical calculations we find that the random-hopping model exhibits Anderson localization at *finite*  $N$ , irrespective of the parity of  $N$ . Moreover, the localization length scales linearly with  $N$ , implying the absence of Anderson localization *only* at  $N = \infty$ . For finite SYK interactions, by performing the exact diagonalization we show that there is a dynamic phase transition from many-body localization to thermal diffusion as interaction strength exceeds a critical value  $J_c$ . In addition, we find that the critical interaction strength  $J_c$  decreases with the increase of  $N$ , consistent with the analytical result of  $J_c/t \propto \frac{1}{N^{5/2} \log N}$  derived from the weakly interacting limit.

**Introduction:** The seminal Sachdev-Ye-Kitaev (SYK) model [1, 2] presents a zero-dimensional (0D) cluster consisting of  $N$  Majorana fermions with random all-to-all interactions. In the large- $N$  limit it is exactly solvable, exhibiting maximal quantum chaos [2–4], emergent  $SL(2, R)$  symmetry as well as a holographic dual to dilaton gravity theory in nearly  $AdS_2$  geometry [2, 3]. Owing to its solvability and intriguing properties, it has stimulated great research interest [5–48]. In particular, the large- $N$  limit of the SYK model, after properly generalized to higher dimensions [35–48], could provide an insightful and promising avenue to investigate the spectral and transport properties of non-Fermi liquid states. Nonetheless, features of the higher-dimensional SYK models with finite  $N$  remain largely unknown. As the case of finite  $N$  is directly relevant to possible experimental realizations [49–52] of SYK models in the future, it is desired to understand the characterizing properties of the higher dimensional SYK models at *finite*  $N$ .

Here we consider a generic SYK chain model of Majorana fermions respecting time-reversal symmetry, which includes four-fermion random interactions and random fermion hopping between neighboring sites as shown in Fig. 1 [see Eq. (1) below]. Note that the neighboring fermion hopping on a bipartite lattice respects the time-reversal symmetry defined as  $\gamma_{j,x} \rightarrow (-)^x \gamma_{j,x}$  where  $\gamma_{j,x}$  represents the Majorana fermion with flavor  $j = 1, \dots, N$  on site  $x$ . Both the random hopping and the random interactions are characterized by Gaussian random variables with mean zero; and their variances are given by  $t^2/N$  and  $3!J^2/N^3$ , respectively. A similar complex fermion version of Eq. (1) was introduced in Ref. [38], where they studied the large- $N$  limit with  $J \gg t$  and showed that it exhibits behaviors of an incoherent metal at high temperature  $T \gg t^2/J$ . In the present paper, we focus on the case of  $J \ll t$  as well as finite  $N$  and investigate its characterizing phase diagram.

We first consider the noninteracting limit, namely  $J = 0$ , for which the model in Eq. (1) reduces to a

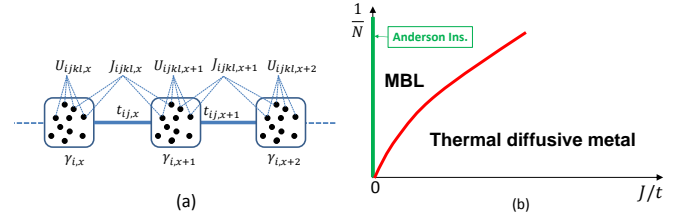


FIG. 1. (a) The schematic representation of the SYK chain model. (b) The global phase diagram of the SYK chain model with finite  $N$ . The system is in the MBL phase when the SYK interaction is relatively weak, but exhibits thermalization and diffusion when the SYK interaction  $J$  exceeds a critical value  $J_c$ . Note that the critical value  $J_c$  decreases with increasing  $N$ .

one-dimensional (1D) random-hopping model [53]. The presence of time-reversal symmetry renders the Majorana system in the BDI class [54, 55]. In particular, when the system size  $L$  is odd, there will be  $N$  zero-energy single-particle modes in the band center due to the particle-hole symmetry. From numerical calculations, we find that the zero modes are localized for finite  $N$  (both even and odd), which implies that all single-particle wavefunctions are Anderson localized. Moreover, our results show that the localization length scales linearly with the fermion flavor  $N$ , i.e.,  $\xi \propto N$ , indicating the absence of Anderson localization *only* at  $N = \infty$ . Inspired by the pioneering work of Refs. [56, 57], we further derive the corresponding supersymmetric field theory and find that the low energy physics can be described by the conventional supersymmetric non-linear  $\sigma$ -model with *vanishing* topological  $\theta$  term. From the supersymmetric field-theory analysis, we obtain that the corresponding conductance decays exponentially with system size and the localization length scales linearly with  $N$ , consistent with the numerical calculations.

For the case of finite interactions, by performing the exact diagonalization (ED) we show that there is a dy-

dynamic phase transition from many-body localized (MBL) phase [58–61] to the thermal diffusive metal phase as the interactions strength exceeds a critical value  $J_c$ . When  $J < J_c$ , the tendency to MBL can be understood perturbatively: a weak interaction is irrelevant to the Anderson localized phase in the noninteracting limit so the system remains many-body localized; namely sufficiently weak SYK interactions cannot effectively thermalize the system which is Anderson localized in the noninteracting limit. Numerically, we find that the dynamic phase transition is characterized by the critical exponent  $\nu \approx 3.4 \pm 0.1$ . To the best of our knowledge, it is the first time in ED calculations to get a critical exponent that is consistent with Harris criteria  $d\nu > 2$  where  $d$  is the spatial dimension [62–64]. Note that the critical exponent obtained here is also consistent with the calculations from real-space renormalization group [65, 66]. Moreover, as shown in Fig. 1b, we find that the critical interaction strength  $J_c$  needed to thermalize the system decreases with the increase of  $N$ , which is consistent with the analytical result of  $J_c/t \propto \frac{1}{N^{5/2} \log N}$  derived from the weakly interacting limit [59].

**The Model:** We consider the SYK chain model of Majorana fermions,

$$\hat{H} = \sum_{x,ij} it_{jk,x} \gamma_{j,x} \gamma_{k,x+1} + \sum_{x,ijkl} \frac{J_{ijkl,x}}{4} \gamma_{i,x} \gamma_{j,x} \gamma_{k,x+1} \gamma_{l,x+1} + \sum_{x,ijkl} U_{ijkl,x} \gamma_{i,x} \gamma_{j,x} \gamma_{k,x} \gamma_{l,x}, \quad (1)$$

where  $\gamma_{j,x}$  labels the Majorana fermion with flavor index  $j=1, \dots, N$  on site  $x=1, \dots, L$ . Here,  $U_{ijkl,x}$  label the usual on-site SYK interactions, while  $t_{jk,x}$  and  $J_{ijkl,x}$  refer to random hopping and interaction between neighboring sites that are Gaussian random variables with mean zero and variance  $\langle t_{jk,x}^2 \rangle = t^2/N$  and  $\langle J_{ijkl,x}^2 \rangle = J^2/N^3$ , respectively. It is obvious that the model in Eq. (1) respects the time-reversal symmetry whose transformation is defined as  $\gamma_{j,x} \rightarrow (-1)^j \gamma_{j,x}$ . By requiring the time-reversal invariance, the onsite quadratic term  $i\gamma_{i,x} \gamma_{j,x}$  is then not allowed in the Hamiltonian above.

In the following, we shall focus on the case of vanishing onsite interactions, namely  $U_{ijkl,x} = 0$ , while varying the nearest-neighbor SYK interaction strength  $J$  with respect to the hopping strength  $t$ . This is partly because the onsite SYK interactions cannot be defined for the case of  $N=2$  Majorana fermions. In contrast, a finite nearest-neighbor SYK interaction  $J$  is allowed for all  $N \geq 2$ , including  $N=2$ . As the case of  $N=2$  is numerically more accessible, we can obtain reliable results up to a reasonably large system size  $L$ . Consequently, we study the phase diagram as a function of  $N$  and  $J/t$  to include the case of  $N=2$ , while setting the onsite interaction to be zero. Nonetheless, we would like to emphasize that the general feature of the global phase diagram does not depend on the specific SYK interactions we consider. In

other words, we expect that characters of the phase diagram obtained for the nearest-neighbor SYK interactions also applies to the case of onsite SYK interactions.

**The non-interacting limit:** In the non-interacting limit, Eq. (1) is equivalent to the random-hopping model with zero-mean amplitude. Although it was shown previously that, when  $N$  is odd, the zero modes in the random-hopping chain with a large non-random diagonal hopping (namely,  $t_{ij,x}$  has a constant diagonal hopping part  $t_0 \delta_{ij}$  in addition to the random hopping part with zero mean) are extended rather than Anderson localized [53, 67–69], it is not clearly known if the random hopping model whose hopping is characterized by zero mean is Anderson localized or not, especially for odd  $N$  Majorana fermions. Thus, to see the situation is different or not from the zero-mean case, we numerically calculate the inverse participation ratio (IPR) [70] of the zero-mode wavefunction, which is defined by

$$\text{IPR} = \frac{\sum_{x=1}^L (\psi_x^* \psi_x)^2}{\left(\sum_{x=1}^L \psi_x^* \psi_x\right)^2}, \quad (2)$$

where  $\psi_x$  labels a zero-mode wavefunction and  $L$  denote the lattice size. Towards the thermodynamic limit, i.e.,  $L \rightarrow \infty$ , the scaling behaviors of the ensemble averaged IPR can tell if the wavefunction is localized (IPR  $\propto \text{const.}$ ), extended ( $\propto \frac{1}{L}$ ), or critical ( $\propto \frac{1}{L^\zeta}$  with  $0 < \zeta < 1$ ). As shown in Fig. 2(a), the IPR saturate to some non-zero constants with increasing the system size for  $N=1, 2, 4$ , signaling a very strong localization behavior.

As a benchmark, we also study the scaling behaviors of the entanglement entropy (EE) of the ground state wavefunction of the random hopping chain. It was shown in Refs. [71, 72] that in the non-interacting system inspecting entanglement properties of the ground state *alone* can tell if the system is localized or not. For the system with  $L = 2\tilde{L} + 1$  sites, we first partition the lattice into two parts (A and B) and then project the lowest  $\tilde{L} + 1$  single-particle eigenstates  $|\psi_l\rangle$  of the Hamiltonian onto one of the subsystems, say, A. According to Klich's method [73], the ground state EE can then be found as  $S = \sum_{l=1}^{\tilde{L}+1} \omega_l \ln \omega_l + (1 - \omega_l) \ln(1 - \omega_l)$ , where  $\omega_l$  stand for the eigenvalues of the Hermitian matrix  $M_{ll'} = \langle P_A \psi_l | P_A \psi_{l'} \rangle$ . As shown in Fig. 2(c), the ground state EE saturates to a constant value as the system size  $L \rightarrow \infty$  for  $N=1, 2, 4$ , clearly implying a localized state.

The scaling behaviors of both the IPR and ground state EE with respect to the system size  $L$  yield consistent results and suggest that the single particle wavefunctions are Anderson-localized in the non-interacting limit, in contrast to the case with constant diagonal hopping [53]. To see if the Anderson localization persists to larger  $N$ , we compute the IPR of the zero modes up to  $N=76$  with fixed system size. The corresponding

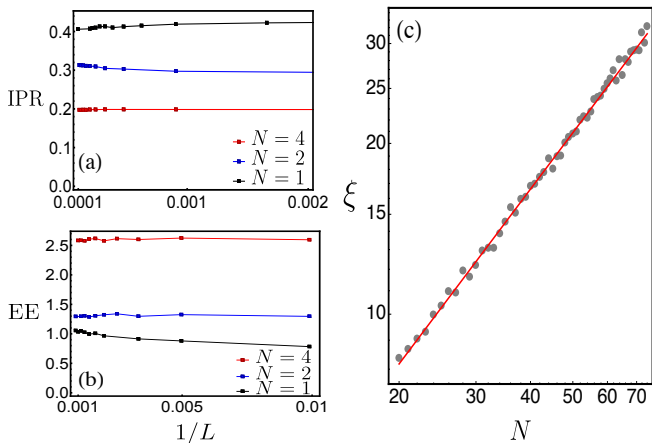


FIG. 2. (a) For  $N = 1, 2, 4$ , we compute both the scaling behavior of disorder averaged IPR (a) and ground state entanglement entropy (EE) (b) with system size  $L$ . The Fermi level is set to zero in computing the EE. (c) The representative linear fit of  $\xi$  with  $N$  for  $N \in [20, 76]$  after 600 disorder realizations with  $L = 6001$ . For clarity, we only show the scaling behavior of one zero mode for each  $N$  and the results for all other zero modes are similar.

localization lengths can be extracted from the relation  $\text{IPR} \propto 1/\xi$  [70]. From the log-log plot shown in Fig. 2(b), we find that the localization length  $\xi$  of  $N \in [20, 76]$  can fit linearly with  $N$ , namely  $\xi \propto N$  for  $N \gg 1$ . It is quite remarkable that a single linear fit works for both even and odd  $N$ ; no discernible sign of parity oscillations can be observed. Note that this linear scaling behavior of localization length holds for all zero-mode wave functions.

Although a similar relation was observed in studies of a different model where the mean value  $t_0$  of hopping amplitudes is finite and even stronger than the variance  $t$  [53, 67, 74], there is an important and qualitative difference between the weak disorder case ( $t \ll t_0$ ) and the present strong disorder case ( $t > 0$  and  $t_0 = 0$  such that  $t/t_0 = \infty$ ). For the case of weak disorder limit ( $t \ll t_0$ ), Anderson localization occurs only for even- $N$  while all wavefunctions are extended for odd- $N$ . Consequently, it is natural to infer that the topological protection of the absence of localization in the wavefunction for odd- $N$  in the weak disorder limit fails in the present strong disorder limit ( $t/t_0 = \infty$ ). Indeed, as we shall show below, the topological  $\theta$  term in the supersymmetric nonlinear- $\sigma$  model has a vanishing coefficient for the present strong-order limit for both even- $N$  and odd- $N$ , which is consistent with the numerical results discussed above.

**Supersymmetric field theory:** To furnish a firm understanding of the numerical results, we develop a field theory model using supersymmetry approach [75–78] which is a very powerful tool in analyzing non-interacting disorder problems. For simplicity, we only sketch the derivation and the details can be found in

the Supplemental Material. Note that, although the supersymmetry method was originally developed to deal with complex fermions, concerning the single particle physics the results of the supersymmetry theory apply for both complex and Majorana fermions as we argue below. Suppose the single particle Hamiltonian for Majorana fermions takes the form of  $H(\gamma) = \sum it_{jk,x} \gamma_{j,x} \gamma_{k,x+1}$ . Imagine there exists an identical “ghost” copy  $H(\gamma')$  of the original  $H(\gamma)$  such that they add up forming the complex fermionic Hamiltonian  $H(\chi) = H(\gamma) + H(\gamma') = \sum_{jk} [it_{jk,x} \chi_{j,x}^\dagger \chi_{k,x+1} + H.c.]$  where  $\chi_j = (\gamma_j^1 + i\gamma_j^2)/2$  are complex fermion annihilation operators. The localization properties of the complex fermion model  $H(\chi)$  is identical to the Majorana fermion model  $H(\gamma)$  as they share the same single-particle matrix  $it_{jk,x}$ .

The basic idea of supersymmetry method is to promote the original anticommuting fermionic field  $\chi$  to the superfield  $\psi$  by adding a commuting bosonic counterpart  $\phi$ , i.e.,  $\psi = (\phi, \chi)^T$ , such that the disorder average can be performed at the very beginning, due to the cancellation of determinants from the Gaussian integrals of complex and Grassmann variables. After the disorder average, the partition function can be written as

$$Z = \int \mathcal{D}(\bar{\psi}, \psi) \exp \left[ i \sum_n \bar{\psi}_{n,\mu} z \psi_{n,\mu} - \frac{2t^2}{N} \sum_{\substack{n \in A \\ m \in B}} \text{str} g_n^{\mu\mu} g_m^{\nu\nu} \right], \quad (3)$$

where summation over repeated indices is assumed,  $z$  is the frequency,  $\text{str}$  represents the supertrace, and  $g_n^{\mu\mu} \equiv \psi_{n,\mu} \otimes \bar{\psi}_{n,\mu}$  is the superfield bilinear living on  $A, B$  sublattices, respectively (for details see the Supplemental Materials). We see that the partition function  $\tilde{Z}$  for the “supersymmetric” Majorana counterpart is the square root of  $Z$  in Eq. (3). Thus, in what follows we shall deal with  $Z$  only. To proceed, we introduce two auxiliary supermatrix fields  $Q_{nm}^\pm \equiv Q_{A,n} \pm iQ_{B,m}$  to decouple the quartic term and then integrate out the superfield  $\psi$  to obtain the action in terms of the superfield  $Q$ . The next step is to get the saddle point solution  $\frac{\delta S}{\delta Q^\pm} = 0$ . Then we perform gradient expansions around the ground state manifold to identify the low energy degrees of freedom. The resulting effective action at  $z = 0$  is

$$S[T] = -\frac{\tilde{\xi}}{8} \int \text{str}(\partial T^{-1} \partial T) dr + S_b, \quad (4)$$

where  $\tilde{\xi} = N$  in unit of the lattice constant  $a$ . Here  $S_b$  denotes the boundary term which depends on the parity of lattice size which is important only if one consider the density of states for an isolated short wire [53].

One key feature of the effective action of Eq. (4) is the absence of the topological term  $(N/2) \text{str} T^{-1} \partial T$  which, according to Refs. [53, 74, 79], would lead to the delocalized zero modes for odd- $N$ . In other words, vanishing topological term in the effective action here implies Anderson localization for both even and odd  $N$ . From the

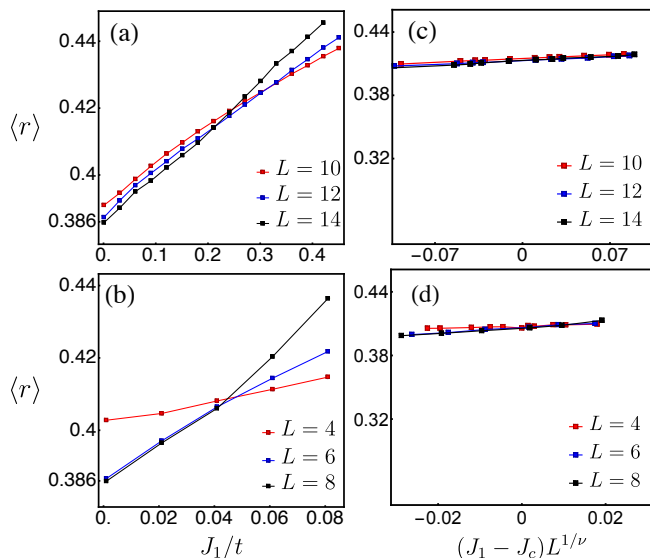


FIG. 3. Disorder averaged level statistics and finite size data collapse for  $N = 2$  (a,c) and  $N = 4$  (b,d). The drift and its slowing down when increasing  $L$  can be seen clearly.  $J_c = 0.2 t, \nu = 3.4$  for  $N = 2$ , and  $J_c = 0.04 t, \nu = 3.2$  for  $N = 4$ . All the results are obtained by setting  $t_1 = 0.5 t, t_2 = 1.5 t$ .

effective action in Eq. (4), it is conceptually straightforward to calculate the physical observables. For instance, the conductance at a given energy  $E$  is the functional average of the corresponding retarded and advanced Green functions  $g(E) \equiv \langle G(E^+)G(E^-) \rangle$ . However, the actual evaluation of conductance using supersymmetric non-linear  $\sigma$ -model is technically heavy and we just show the result here. Using the transfer matrix method [53], we obtain the conductance  $g$  at zero energy for  $L \gg \xi$ :

$$g \approx \sqrt{\frac{\tilde{\xi}}{\pi L}} \exp \left[ -\frac{L}{\tilde{\xi}} \right], \quad (5)$$

which is consistent with the numerically observed Anderson localization behavior. Moreover, from Eq. (5), it is clear that the coupling constant  $\tilde{\xi}$  in the effective action of Eq. (4) can be identified as the localization length, which scales linearly with  $N$  for  $N \gg 1$ . This linear- $N$  localization length for  $N \gg 1$  is consistent with the result obtained from numerical calculations.

**Finite SYK interactions:** After establishing Anderson localization in the non-interacting limit, we are ready to consider finite interaction strength, i.e.,  $J > 0$ . To investigate how the interactions can thermalize the system, we employ ED to calculate the many-body level statistics of the interacting Hamiltonian of Majorana fermions in Eq. (1). Assuming that  $\{e_n\}$  denotes the many-body energy level in an ascending order, we calculate the dimensionless ratio  $\tilde{r}_n$  defined by  $\tilde{r}_n = \frac{\min(s_n, s_{n-1})}{\max(s_n, s_{n-1})}$ , where  $s_n = e_{n+1} - e_n$  [60, 80]. For the uncorrelated energy levels obeying Poisson distribution,  $\langle \tilde{r} \rangle \rightarrow 2 \ln 2 - 1 \approx 0.386$ ;

while for the Gaussian orthogonal ensemble (GOE) of random matrix,  $\langle \tilde{r} \rangle \rightarrow 0.53$ . When  $J=0$ ,  $\langle \tilde{r} \rangle \approx 0.386$  for  $N=2$  and  $N=4$ , as shown in Fig. 3(a) and (b) respectively, indicating Poisson distribution that is consistent with the Anderson localized state for finite  $N$ . Moreover,  $\langle \tilde{r} \rangle$  increases as  $J$  increases, indicating that the SYK interactions tend to thermalize the system. For both  $N=2$  and  $N=4$ , it is clear that  $\langle \tilde{r} \rangle$  between adjacent system sizes  $L$  crosses at a critical interaction strength  $J_c$ , indicating there is a dynamic quantum phase transition from the MBL phase ( $J < J_c$ ) to the thermalized phase ( $J > J_c$ ). Due to the finite size effect, the crossing points drift gradually towards smaller  $J_c$  as  $L$  increases, which is common in the ED studies of many-body localizations [60]. Nonetheless, the tendency of the drift becomes slower for larger  $L$ . Essentially, this implies that  $J_c$  is nonzero and the MBL phase should persist below  $J_c$  in the thermodynamic limit.

To characterize the MBL transitions, we explore the critical behaviors of the dynamic transition. Around the MBL transition,  $\langle \tilde{r} \rangle$  should obey a universal scaling function, i.e.,  $\langle \tilde{r} \rangle = f \left[ \frac{|J - J_c|}{L^{1/\nu}} \right]$ , where  $\nu$  is the correlation/localization length critical exponent. By collapsing the data, as shown in Fig. 3(c), we obtain the critical exponent  $\nu \approx 3.4 \pm 0.1$  for  $N=2$ . (for  $N=4$ , the data collapse shown in Fig. 3(d) gives rise to  $\nu \approx 3.2 \pm 0.2$ ). Remarkably, the obtained exponent is consistent with Harris criteria  $d\nu > 2$  [62–64] where  $d=1$  is the spatial dimension of the system. To the best of our knowledge, it is the first time from ED calculations to obtain a critical exponent  $\nu$  consistent with Harris criteria  $d\nu > 2$  [62–64]. One important ingredient of obtaining this consistent critical exponent is that we manage to reduce the finite-size effect in the ED calculations by considering a dimerized version of Eq. (1), i.e., we set the variance to be  $t_1^2/N$  and  $t_2^2/N$ ,  $t_1 \neq t_2$ , for odd and even bonds, respectively. The staggered variances can significantly shorten the localization length (which is still proportional to  $N$ , see Supplemental Material.); accordingly, the finite-size effect decreases for the accessible system size.

As explicitly shown for the  $N=2$  and  $N=4$  SYK chain, the finite- $N$  effect renders MBL when the interaction strength  $J$  is smaller than a critical value  $J_c$ . The value of  $J_c$  of  $N=4$  is smaller than the one of  $N=2$ , indicating that  $J_c$  decreases as  $N$  increases. Due to the absence of Anderson localization for  $N = \infty$ , it is clear that  $J_c = 0$  for  $N = \infty$ . As the discussion of the SYK models generally relies on a large- $N$  approximation to control the quantum fluctuations, it is interesting to further explore how the critical strength  $J_c$  scale with  $1/N$ . In the weakly interacting limit, the energy scale corresponding to the MBL transition is given by  $T_c \sim \frac{\delta_\xi}{\lambda |\log \lambda|}$  [58, 59], where  $\delta_\xi = \frac{1}{\rho \xi}$  is the average level spacing of single-particle states within a localization length in the non-interacting limit,  $\rho$  is the average density of single-particle states per unit volume

(namely unit length for the present SYK chain), and the dimensionless quantity  $\lambda = \frac{J}{N^{3/2}\delta_\xi}$  characterizes the interaction strength with respect to the average single-particle level spacing. It is known from the noninteracting calculations that  $\xi \propto N$  and the average density of states per unit volume is supposed to be  $\rho \propto t^{-1}N$  (see Supplemental Material), thus  $\delta_\xi \propto tN^{-2}$  and  $T_c \propto \frac{t^2}{J} \frac{1}{N^{5/2} \log N}$ . It directly leads to a rough estimate of the critical interaction strength  $J_c/t \propto \frac{1}{N^{5/2} \log N}$  for the dynamic transition of full many-body localization (namely requiring  $T_c \sim t$  where  $t$  is the order of the bandwidth). By using the numerical data shown in Fig. 3, we estimate that the critical strength scales as  $J_c \propto N^{-\eta}$  with  $\eta \approx 2.3$ , which is close to the scaling behavior of  $\eta = 5/2$  derived from the weakly interacting limit (up to a logarithmic correction). Note that this scaling is consistent with the requirement that  $J_c$  vanishes at  $N = \infty$ .

**Discussion and concluding remarks:** We have shown that, in the non-interacting limit, all the single particle states in the SYK chain model with finite  $N$  are localized irrespective to the parity of  $N$ , due to the vanishing topological  $\theta$ -term. Here we speculate that the same localization physics also applies to the other four symmetry classes in 1D based on the notion of *superuniversality*, [74, 79, 81] which refers to the fact that in 1D, all five symmetry classes, including class D, DIII, and other three chiral classes, share the similar low-energy properties. We further showed that the system enters an MBL phase for weak SYK interactions but undergoes a dynamic quantum phase transition from MBL to a thermalized phase when the interactions exceed a critical strength  $J_c$  with  $J_c/t \sim \frac{1}{N^{5/2} \log N}$ . Our ED calculations show that the critical exponent  $\nu \approx 3.4$ , which is consistent with the Harris criteria [62–64]. It is remarkable that the critical exponent is close to the value  $\nu \approx 3.5 \pm 0.3$  obtained from real-space renormalization group calculations [66]. Finally, let's mention some future directions related to finite- $N$ . For instance, it would be desired to characterize the thermal phase at finite- $N$  in full details including its Lyapunov exponent, specific heat, and transport behaviors. Due to the finite- $N$  effect, it is expected that its characters should be renormalized from its large- $N$  limit.

*Acknowledgment.*— We would like to thank Y.-F. Gu and X.-L. Qi for helpful discussions. This work is supported in part by the MOST of China under Grant No. 2016YFA0301001 (H.Y.) and the NSFC under Grant No. 11474175 (X.D., S.-K.J., and H.Y.).

---

\* yaohong@tsinghua.edu.cn

[1] S. Sachdev and J. Ye, *Phys. Rev. Lett.* **70**, 3339 (1993).  
 [2] A. Kitaev, A simple model of quantum holography (unpublished) (2015).

- [3] J. Maldacena and D. Stanford, *Phys. Rev. D* **94**, 106002 (2016).  
 [4] J. Maldacena, S. H. Shenker, and D. Stanford, *J. High Energy Phys.* **2016**, 106 (2016).  
 [5] J. Polchinski and V. Rosenhaus, *J. High Energy Phys.* **2016**, 1 (2016).  
 [6] W. Fu and S. Sachdev, *Phys. Rev. B* **94**, 035135 (2016).  
 [7] Z. Bi, C.-M. Jian, Y.-Z. You, K. A. Pawlak, and C. Xu, *Phys. Rev. B* **95**, 205105 (2017).  
 [8] S. Banerjee and E. Altman, *Phys. Rev. B* **95**, 134302 (2017).  
 [9] A. M. García-García and J. J. M. Verbaarschot, *Phys. Rev. D* **94**, 126010 (2016).  
 [10] J. S. Cotler, G. Gur-Ari, M. Hanada, J. Polchinski, P. Saad, S. H. Shenker, D. Stanford, A. Streicher, and M. Tezuka, *J. High Energy Phys.* **2017**, 118 (2017).  
 [11] A. M. García-García and J. J. M. Verbaarschot, *Phys. Rev. D* **96**, 066012 (2017).  
 [12] Y. Chen, H. Zhai, and P. Zhang, *J. High Energy Phys.* **2017**, 150 (2017).  
 [13] D. Bagrets, A. Altland, and A. Kamenev, *Nucl. Phys. B* **921**, 727 (2017).  
 [14] D. Khveshchenko, [arXiv:1705.03956](https://arxiv.org/abs/1705.03956) (2017).  
 [15] A. Eberlein, V. Kasper, S. Sachdev, and J. Steinberg, *Phys. Rev. B* **96**, 205123 (2017).  
 [16] J. Sonner and M. Vielma, *J. High Energy Phys.* **2017**, 149 (2017).  
 [17] Y. Gu, A. Lucas, and X.-L. Qi, *J. High Energy Phys.* **2017**, 120 (2017).  
 [18] C. Liu, X. Chen, and L. Balents, [arXiv:1709.06259](https://arxiv.org/abs/1709.06259) (2017).  
 [19] Y. Huang and Y. Gu, [arXiv:1709.09160](https://arxiv.org/abs/1709.09160) (2017).  
 [20] A. Kitaev and S. J. Suh, [arXiv:1711.08467](https://arxiv.org/abs/1711.08467) (2017).  
 [21] Y. Jia, J. J. Verbaarschot, *et al.*, [arXiv:1801.02696](https://arxiv.org/abs/1801.02696) (2018).  
 [22] A. M. García-García and M. Tezuka, [arXiv:1801.03204](https://arxiv.org/abs/1801.03204) (2018).  
 [23] G. Tarnopolsky, [arXiv:1801.06871](https://arxiv.org/abs/1801.06871) (2018).  
 [24] J. Maldacena, D. Stanford, and Z. Yang, *Progress of Theoretical and Experimental Physics* **2016** (2016).  
 [25] K. Jensen, *Phys. Rev. Lett.* **117**, 111601 (2016).  
 [26] J. Engelsöy, T. G. Mertens, and H. Verlinde, *J. High Energy Phys.* **2016**, 139 (2016).  
 [27] D. J. Gross and V. Rosenhaus, *J. High Energy Phys.* **2017**, 92 (2017).  
 [28] A. Jevicki and K. Suzuki, *J. High Energy Phys.* **2016**, 46 (2016).  
 [29] S. R. Das, A. Ghosh, A. Jevicki, and K. Suzuki, [arXiv:1711.09839](https://arxiv.org/abs/1711.09839) (2017).  
 [30] S. R. Das, A. Ghosh, A. Jevicki, and K. Suzuki, [arXiv:1712.02725](https://arxiv.org/abs/1712.02725) (2017).  
 [31] J. A. Das, Sumit R. and K. Suzuki, *J. High Energy Phys.* **2017**, 17 (2017).  
 [32] R.-G. Cai, S.-M. Ruan, R.-Q. Yang, and Y.-L. Zhang, [arXiv:1709.06297](https://arxiv.org/abs/1709.06297) (2017).  
 [33] S.-K. Jian, Z.-Y. Xian, and H. Yao, [arXiv:1709.02810](https://arxiv.org/abs/1709.02810) (2017).  
 [34] M. Blake, H. Lee, and H. Liu, [arXiv:1801.00010](https://arxiv.org/abs/1801.00010) (2018).  
 [35] Y. Gu, X.-L. Qi, and D. Stanford, *J. High Energy Phys.* **2017**, 125 (2017).  
 [36] R. A. Davison, W. Fu, A. Georges, Y. Gu, K. Jensen, and S. Sachdev, *Phys. Rev. B* **95**, 155131 (2017).  
 [37] A. Lucas, Y. Gu, and X.-L. Qi, *SciPost Physics* **2**, 018 (2017).

- [38] X.-Y. Song, C.-M. Jian, and L. Balents, *Phys. Rev. Lett.* **119**, 216601 (2017).
- [39] M. Berkooz, P. Narayan, M. Rozali, and J. Simón, *J. High Energy Phys.* **2017**, 138 (2017).
- [40] S.-K. Jian and H. Yao, *Phys. Rev. Lett.* **119**, 206602 (2017).
- [41] C.-M. Jian, Z. Bi, and C. Xu, *Phys. Rev. B* **96**, 115122 (2017).
- [42] X. Chen, R. Fan, Y. Chen, H. Zhai, and P. Zhang, *Phys. Rev. Lett.* **119**, 207603 (2017).
- [43] P. Zhang, [arXiv:1707.09589](https://arxiv.org/abs/1707.09589).
- [44] W. Cai, X.-H. Ge, and G.-H. Yang, [arXiv:1711.07903](https://arxiv.org/abs/1711.07903) (2017).
- [45] A. M. García-García, A. Romero-Bermúdez, and M. Tezuka, [arXiv:1707.02197](https://arxiv.org/abs/1707.02197) (2017).
- [46] A. A. Patel, J. McGreevy, D. P. Arovas, and S. Sachdev, [arXiv:1712.05026](https://arxiv.org/abs/1712.05026) (2017).
- [47] D. Chowdhury, Y. Werman, E. Berg, and T. Senthil, [arXiv:1801.06178](https://arxiv.org/abs/1801.06178) (2018).
- [48] X. Wu, X. Chen, C.-M. Jian, Y.-Z. You, and C. Xu, [arXiv:1802.04293](https://arxiv.org/abs/1802.04293) (2018).
- [49] I. Danshita, M. Hanada, and M. Tezuka, *Progress of Theoretical and Experimental Physics* **2017**, 083101 (2017).
- [50] D. I. Pikulin and M. Franz, *Phys. Rev. X* **7**, 031006 (2017).
- [51] A. Chew, A. Essin, and J. Alicea, *Phys. Rev. B* **96**, 121119 (2017).
- [52] Z. Luo, Y.-Z. You, J. Li, C.-M. Jian, D. Lu, C. Xu, B. Zeng, and R. Laflamme, [arXiv:1712.06458](https://arxiv.org/abs/1712.06458) (2017).
- [53] A. Altland and R. Merkt, *Nucl. Phys. B* **607**, 511 (2001).
- [54] A. Kitaev, in *AIP Conference Proceedings*, Vol. 1134 (AIP, 2009) pp. 22–30.
- [55] S. Ryu, A. P. Schnyder, A. Furusaki, and A. W. Ludwig, *New Journal of Physics* **12**, 065010 (2010).
- [56] A. Altland and B. Simons, *Nucl. Phys. B* **562**, 445 (1999).
- [57] A. Altland and B. Simons, *Journal of Physics A: Mathematical and General* **32**, L353 (1999).
- [58] I. V. Gornyi, A. D. Mirlin, and D. G. Polyakov, *Phys. Rev. Lett.* **95**, 206603 (2005).
- [59] D. Basko, I. Aleiner, and B. Altshuler, *Annals of physics* **321**, 1126 (2006).
- [60] V. Oganesyan and D. A. Huse, *Phys. Rev. B* **75**, 155111 (2007).
- [61] R. Nandkishore and D. A. Huse, *Annu. Rev. Condens. Matter Phys.* **6**, 15 (2015).
- [62] A. B. Harris, *Journal of Physics C: Solid State Physics* **7**, 1671 (1974).
- [63] J. T. Chayes, L. Chayes, D. S. Fisher, and T. Spencer, *Phys. Rev. Lett.* **57**, 2999 (1986).
- [64] A. Chandran, C. R. Laumann, and V. Oganesyan, [arXiv:1509.04285](https://arxiv.org/abs/1509.04285) (2015).
- [65] R. Vosk, D. A. Huse, and E. Altman, *Phys. Rev. X* **5**, 031032 (2015).
- [66] A. C. Potter, R. Vasseur, and S. A. Parameswaran, *Phys. Rev. X* **5**, 031033 (2015).
- [67] P. W. Brouwer, C. Mudry, B. D. Simons, and A. Altland, *Phys. Rev. Lett.* **81**, 862 (1998).
- [68] L. Balents and M. P. A. Fisher, *Phys. Rev. B* **56**, 12970 (1997).
- [69] P. W. Brouwer, C. Mudry, and A. Furusaki, *Phys. Rev. Lett.* **84**, 2913 (2000).
- [70] S. Johri and R. N. Bhatt, *Phys. Rev. Lett.* **109**, 076402 (2012).
- [71] M. Pournavari and K. Yang, *Phys. Rev. B* **88**, 075123 (2013).
- [72] M. Pournavari and K. Yang, *Phys. Rev. B* **89**, 115104 (2014).
- [73] I. Klich, *Journal of Physics A* **39**, L85 (2006).
- [74] A. Altland, D. Bagrets, and A. Kamenev, *Phys. Rev. B* **91**, 085429 (2015).
- [75] K. Efetov, *Supersymmetry in disorder and chaos* (Cambridge University Press, 1999).
- [76] A. D. Mirlin, *Physics Reports* **326**, 259 (2000).
- [77] A. Altland, C. Offer, and B. Simons, in *Supersymmetry and Trace Formulae* (Springer, 1999) pp. 17–57.
- [78] F. Wegner, *Supermathematics and Its Applications in Statistical Physics: Grassmann Variables and the Method of Supersymmetry*, Vol. 920 (Springer, 2016).
- [79] A. Altland, D. Bagrets, L. Fritz, A. Kamenev, and H. Schmiedt, *Phys. Rev. Lett.* **112**, 206602 (2014).
- [80] Y. Y. Atas, E. Bogomolny, O. Giraud, and G. Roux, *Phys. Rev. Lett.* **110**, 084101 (2013).
- [81] I. A. Gruzberg, N. Read, and S. Vishveshwara, *Phys. Rev. B* **71**, 245124 (2005).

## SUPPLEMENTAL MATERIALS

### A. Derivation of supersymmetric field theory

#### 1. Disorder average

The derivation of the supersymmetric field theory largely follows the approach developed in Refs. [53, 56, 74]. The hopping matrix elements satisfies

$$\langle t_{nm}^{\mu\nu} \rangle = 0, \quad (\text{S1})$$

$$\langle t_{nm}^{\mu\nu} t_{nm}^{\nu'\mu'} \rangle = \frac{\lambda^2}{N} \delta_{\mu\mu'} \delta_{\nu\nu'} \delta_{m,n+1}. \quad (\text{S2})$$

In order to carry out the disorder average, we promote the fermionic field  $\phi$  to the 2-component superfield

$$\psi = \begin{pmatrix} \psi_b \\ \psi_f \end{pmatrix} \quad (\text{S3})$$

with the subscripts  $b, f$  denote the bosonic and fermionic field variables, respectively. Then we can proceed by integrating over  $t$ ,

$$\begin{aligned} & \left\langle \exp \left( i \sum_{n \in A, m \in B, \mu\nu} \bar{\psi}_{n,\mu} t_{nm}^{\mu\nu} \psi_{m,\nu} + h.c. \right) \right\rangle = \mathcal{C} \int dt \exp \left( i \sum_{n \in A, m \in B, \mu\nu} \bar{\psi}_{n,\mu} t_{nm}^{\mu\nu} \psi_{m,\nu} + h.c. - \frac{N}{2\lambda^2} \text{Tr } t^2 \right) \\ & = \mathcal{C} \int dt \exp \left( - \sum_{n \in A, m \in B, \mu\nu} \left| \sqrt{\frac{N}{2}} \frac{1}{\lambda} t_{nm}^{\mu\nu} - i\lambda \sqrt{\frac{2}{N}} \bar{\psi}_{n,\mu} \psi_{m,\nu} \right|^2 \right) = \exp \left( - \sum_{n \in A, m \in B, \mu\nu} \frac{2\lambda^2}{N} \bar{\psi}_{n,\mu} \psi_{m,\nu} \bar{\psi}_{m,\nu} \psi_{n,\mu} \right) \\ & = \exp \left( - \sum_{n \in A, m \in B, \mu\nu} \frac{2\lambda^2}{N} \psi_{n,\mu} \bar{\psi}_{n,\mu} \psi_{m,\nu} \bar{\psi}_{m,\nu} \right) = \exp \left( - \frac{2\lambda^2}{N} \sum_{n \in A, m \in B, \mu\nu} \text{str } g_n^{\mu\mu} g_m^{\nu\nu} \right) \end{aligned} \quad (\text{S4})$$

with  $\mathcal{C}$  being a normalization constant. And we have introduced the bilinear term

$$g_n^{\mu\mu} \equiv \psi_{n,\mu} \otimes \bar{\psi}_{n,\mu} \quad (\text{S5})$$

In the last two identities of Eq. (S4) we have made use of the cyclic invariance property of the supertrace [78]. Then we arrive at the partition function Eq. (3) in the main text.

### 2. Hubbard-Stratonovich transformation

Now we perform the Hubbard-Stratonovich transformation by introducing a pair of supermatrix fields  $Q_{nm}^\pm \equiv Q_{A,n} \pm iQ_{B,m}$ , with  $Q_{A,n}$  ( $Q_{B,m}$ ) lives on  $A$  ( $B$ ) sublattice, respectively.

$$\begin{aligned} Z & = \int \mathcal{D}(\bar{\psi}, \psi) \exp \left( i \sum_{n,\mu} \bar{\psi}_{n,\mu} z \psi_{n,\mu} - \frac{2\lambda^2}{N} \sum_{n \in A, m \in B, \mu\nu} \text{str } g_n^{\mu\mu} g_m^{\nu\nu} \right) \\ & \times \int \mathcal{D}Q^\pm \exp \left( - \sum_{n \in A, m \in B, \mu\nu} \left( \frac{1}{\lambda} \sqrt{\frac{1}{2N}} Q^- - i\lambda \sqrt{\frac{2}{N}} \psi_{n,\mu} \bar{\psi}_{n,\mu} \right) \left( \frac{1}{\lambda} \sqrt{\frac{1}{2N}} Q^+ - i\lambda \sqrt{\frac{2}{N}} \psi_{m,\nu} \bar{\psi}_{m,\nu} \right) \right) \\ & = \int \mathcal{D}Q^\pm \mathcal{D}(\bar{\psi}, \psi) \exp \left( i \sum_{n,\mu} \bar{\psi}_{n,\mu} z \psi_{n,\mu} + \frac{i}{N} \sum_{n \in A, \mu\nu} \bar{\psi}_{n,\mu} (Q_{n,n-1}^+ + Q_{n,n+1}^+) \psi_{n,\mu} \right. \\ & \left. + \frac{i}{N} \sum_{m \in B, \mu\nu} \bar{\psi}_{m,\nu} (Q_{m,m-1}^- + Q_{m,m+1}^-) \psi_{m,\nu} - \frac{N}{2\lambda^2} \sum_{n \in A, m \in B} Q_{nm}^+ Q_{mn}^- \right) \end{aligned} \quad (\text{S6})$$

The next step is to integrate out  $\psi$  and we arrive at

$$S[Q^\pm] = \frac{N}{2t^2} \sum_n \text{str}(Q^+ Q^-) - N \sum_{n \in A} \text{str} \ln(z + Q_{n,n+1}^+ + Q_{n,n-1}^+) - N \sum_{m \in B} \text{str} \ln(z + Q_{m,m+1}^- + Q_{m,m-1}^-). \quad (\text{S7})$$

### 3. The non-linear $\sigma$ -model in the strongly disordered limit

It is clear that, for  $z = 0$ , the action in Eq. (S7) is invariant under the transformation  $Q^+ \rightarrow T_1 Q^+ T_2$  and  $Q^- \rightarrow T_2^{-1} Q^- T_1^{-1}$ , where  $T_1, T_2 \in \text{GL}(1|1)$ , and  $\text{GL}(1|1)$  is the generalization of the original fermionic symmetry.

The overall factor  $N$  enables us to seek the saddle point solution which is exact in the large- $N$  limit. By assuming a uniform ansatz  $Q^\pm = \frac{1}{2}(Q_{n,n+1}^\pm + Q_{n,n-1}^\pm)$ , from the saddle point condition ( $\frac{\delta S}{\delta Q^\pm} = 0$ ) we obtain

$$Q^\mp = \frac{2\lambda^2}{z + Q^\mp} \implies Q_{\text{sp}}^\pm = \frac{1}{2} \left( -z \pm \sqrt{z^2 + 8\lambda^2} \right). \quad (\text{S8})$$

To identify the low energy degrees of freedom for  $z = 0$ , we can parameterize  $Q^\pm$  by  $(Q^+, Q^-) = (PT, T^{-1}P)$  in Eq. (S7), where both  $T, P \in \text{GL}(1|1)$  and  $T$  stands for massless fluctuation while  $P$  is the massive fluctuation that is incompatible with the symmetry of the ground state.

Let's ignore the massive fluctuations by setting  $P = \mathbb{1}$ , the action is of the form,

$$S_{\text{fl}}[T] = N \sum_{n \in A} \text{str} \ln (T_{n,n+1} + T_{n,n-1}) + N \sum_{m \in B} \text{str} \ln (T_{m,m+1}^{-1} + T_{m,m-1}^{-1}). \quad (\text{S9})$$

we then expand  $T_{nm}$  as

$$T_{nm} = T_n + \frac{a}{2} \partial_{n,m} T_n + \frac{a^2}{8} \partial_{n,m}^2 T_n + \dots \quad (\text{S10})$$

where  $a$  is the lattice constant and  $\partial_{n,m}$  denote the directional derivative from site  $n \rightarrow m$ . Taking Eq. (S10) into Eq. (S9),

$$\begin{aligned} \frac{1}{N} S_{\text{fl}}[T] &\approx \sum_{n \in A} \text{str} \ln \left( 2T_n + \frac{a}{2} \partial_{n,n+1} T_n + \frac{a}{2} \partial_{n,n-1} T_n + \frac{a^2}{8} \partial_{n,n+1}^2 T_n + \frac{a^2}{8} \partial_{n,n-1}^2 T_n \right) \\ &+ \sum_{m \in B} \text{str} \ln \left( 2T_m^{-1} + \frac{a}{2} \partial_{m,m+1} T_m^{-1} + \frac{a}{2} \partial_{m,m-1} T_m^{-1} + \frac{a^2}{8} \partial_{m,m+1}^2 T_m^{-1} + \frac{a^2}{8} \partial_{m,m-1}^2 T_m^{-1} \right) \\ &\approx \sum_{n \in A} \text{str} \ln 2T_n - \sum_{m \in B} \text{str} \ln 2T_m + \frac{a^2}{16} \sum_{n \in A} (T_n^{-1} \partial_{n,n+1}^2 T_n + T_n^{-1} \partial_{n,n-1}^2 T_n) + \frac{a^2}{16} \sum_{m \in B} (T_m \partial_{m,m+1}^2 T_m^{-1} + T_m \partial_{m,m-1}^2 T_m^{-1}) \\ &\approx \frac{a^2}{16} \sum_{n \in A} (T_n^{-1} \partial_{n,n+1}^2 T_n + T_n^{-1} \partial_{n,n-1}^2 T_n) + \frac{a^2}{16} \sum_{m \in B} (T_m \partial_{m,m+1}^2 T_m^{-1} + T_m \partial_{m,m-1}^2 T_m^{-1}), \end{aligned} \quad (\text{S11})$$

where we have made use of the fact that  $\sum_{m \in B} \partial_{n,m} T_n = 0$ . By taking the continuum limit  $\sum_{n \in A} \rightarrow \frac{1}{2a} \int$ , Eq. (S11) can be written as

$$\begin{aligned} S_{\text{fl}}[T] &= \frac{Na^2}{8} \left( \sum_{n \in A} \text{str}(T_n^{-1} \partial^2 T_n) + \sum_{m \in B} \text{str}(T_m \partial^2 T_m^{-1}) \right) \\ &\simeq \frac{Na}{16} \int \text{str} (T^{-1} \partial^2 T + T \partial^2 T^{-1}) = -\frac{Na}{8} \int \text{str}(\partial T^{-1} \partial T). \end{aligned} \quad (\text{S12})$$

where the integration by parts is used in the last equality.

## B. Level statistics at large $J$

As shown in Fig. S4, as  $J_1$  increases,  $\langle r \rangle$  for both  $N = 2$  and  $N = 4$  increase towards the GOE value 0.531.

## C. Density of States and localization length in the non-interacting limit

In the non-interacting limit, there are  $N \times L$  single particle states in total. Therefore the single particle density of states  $\rho$  per unit length can be found as

$$\rho = \frac{NL}{L} \frac{1}{\Delta E} = \frac{N}{\Delta E}, \quad (\text{S13})$$

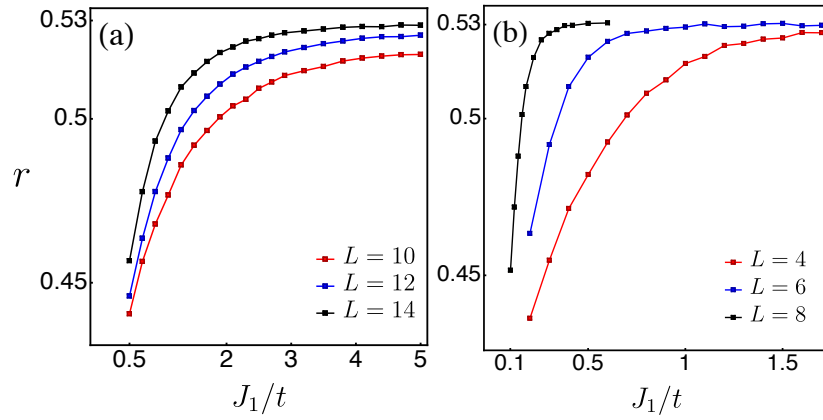


FIG. S4. Level statistics at large  $J_1$  for  $N = 2$  (a) and  $N = 4$  (b).

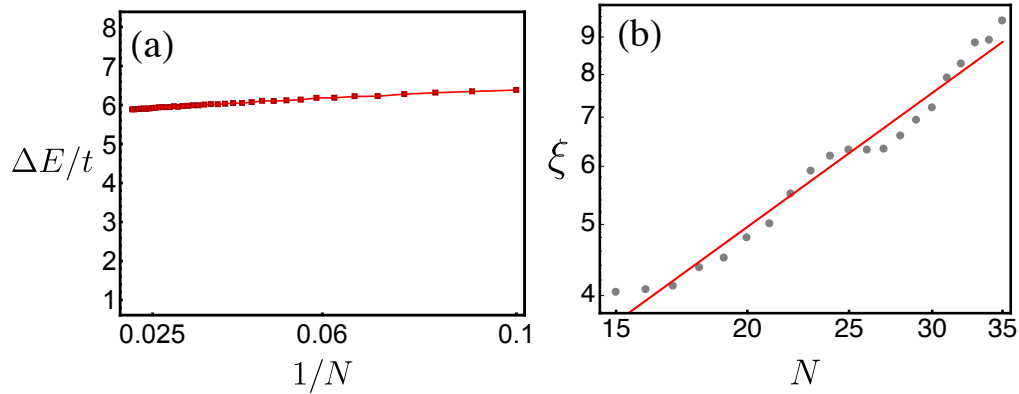


FIG. S5. (a)  $\Delta E$  as a function of  $1/N$  with  $N \in [10, 48]$ . (b) Log-log plot for the localization length  $\xi$  as a function of  $N$  with  $N \in [15, 35]$ . The system size  $L = 1001$ . All the results are obtained by setting  $t_1 = 0.5 t$ ,  $t_2 = 1.5 t$ .

where  $\Delta E$  is the total bandwidth. As shown in Fig. S5(a),  $\Delta E/t$  saturates to constant as  $N \rightarrow \infty$  with fixed  $L$ . So we conclude  $\rho \propto t^{-1}N$ .

In addition, we also compute the localization length  $\xi$  in the presence of dimerization. The data shown in Fig. S5(b) gives rise to  $\xi \approx 0.22N^\alpha$  with  $\alpha = 1.04 \pm 0.04$ . While in the uniform case mentioned in the main text we have  $\xi \approx 0.38N^{1.02 \pm 0.02}$ . So we find in both cases  $\xi$  always scales linearly with  $N$  and the dimerization effectively shortens  $\xi$ .